The Journal of Experimental Biology 207, 1585-1596
Published by The Company of Biologists 2004
doi:10.1242/jeb.00922

The hydrodynamic trails of *Lepomis gibbosus* (Centrarchidae), *Colomesus psittacus* (Tetraodontidae) and *Thysochromis ansorgii* (Cichlidae) investigated with scanning particle image velocimetry

Wolf Hanke* and Horst Bleckmann

Institut für Zoologie der Rheinischen Friedrich-Wilhelms-Universität Bonn, Poppelsdorfer Schloß, D-53115 Bonn, Germany

*Author for correspondence at present address: Allgemeine Zoologie und Neurobiologie, Ruhr-Universität Bochum, ND 6/33, 44780 Bochum, Germany (e-mail: hanke@neurobiologie.ruhr-uni-bochum.de)

Accepted 4 February 2004

Summary

The hydrodynamic trails of fish belonging to the families Centrarchidae, Tetraodontidae and Cichlidae were investigated. Water movements were measured in six horizontal planes, spaced 10–12 mm apart, for up to 5 min after the passage of a fish, using a computer controlled array of modulated laser diodes. We measured continuously and non-continuously swimming fish. Water velocities decayed rapidly in the leading seconds after the passage of a fish, but could still be measured for a period considerably longer than that. In still water (median water velocity <0.5 mm s^{-1}), the hydrodynamic trails of *Lepomis gibbosus* lasted for more than 5 min. The trails of *Colomesus psittacus* and *Thysochromis ansorgii* could be detected for more than 30 s and more than 3 min, respectively. The water disturbance left behind by these fish was sufficient to be sensed by a piscivorous predator at a distance where vision or hearing frequently fail. Acoustic stimuli estimated from a dipole model in a distance that would be covered by the tested fish in 1 min (4–25 m) were 1.5×10^{-7} to 3.1×10^{-10} m s^{-2}, while the hearing threshold of a perch is three orders of magnitude above that. By contrast, the fish wakes after 1 min (except for one *Colomesus* wake) contained water velocities between 0.95 and 2.05 mm s^{-1}, which are within the detection range of hydrodynamic sensory systems. The three species differed with respect to water velocities, the spatial extent of the fish-generated water disturbances and the structure of the wake.

Key words: wake following, lateral line, hydrodynamic reception, particle image velocimetry (PIV), *Lepomis*, *Colomesus*, *Thysochromis*.

Introduction

Most aquatic animals have hydrodynamic receptor systems (Bleckmann, 1994). They use these systems for rheotaxis (Baker and Montgomery, 2002), the detection of surface waves (Bleckmann et al., 1989), and the detection of midwater hydrodynamic events such as those caused by predators, conspecifics or prey (Bleckmann, 1994). Harbour seals *Phoca vitulina* can track hydrodynamic trails of moving objects with their vibrissae over a distance where vision and hearing should fail (Dehnhardt et al., 2001). European catfish *Silurus glanis* can follow the swim paths of their prey, which suggests hydrodynamic or chemical trail-following (Pohlmann et al., 2001). Despite recent advances in the investigation of the behavioural functions of the lateral line and the peripheral and central processing of hydrodynamic sensory information by fish (e.g. Bleckmann et al., 2001), and the sensory abilities of seals (Dehnhardt et al., 2001), data on the information contained in animal-caused water motions, i.e. their frequency content, three-dimensional extension and especially their ageing, are still rare.

In this study, we used scanning digital particle image velocimetry (S-DPIV) to measure the hydrodynamic trails caused by swimming fish of three teleost species. While classical digital particle image velocimetry (DPIV) measures velocities in a single layer of fluid illuminated by a laser light sheet (Adrian, 1991; Westerweel, 1997; Drucker and Lauder, 2001, 2003), S-DPIV measures velocities in multiple layers using one measurement, by scanning the laser light through various planes. The result is an extension of the velocity information from a single layer to a volume.

DPIV has been applied to the water motions caused by moving animals (Stamhuis and Videler, 1995; Müller et al., 1997, 2000; Drucker and Lauder, 2000, 2001). Drucker and Lauder (1999) reconstructed three-dimensional information from successive two-dimensional PIV measurements. Nauen and Lauder (2002) measured three-dimensional velocity information in a water layer behind a swimming trout using the stereoscopic information from two high-speed cameras. Drucker and Lauder (2003) investigated the flow caused by salmonid pectoral fins using DPIV. The above studies focussed

on the function of fish fins and body movements, their role in propulsion, steering and braking and the fluid forces. None of these studies attempted to investigate the long-term development of fish-generated wakes.

Hanke et al. (2000) showed that the hydrodynamic wake of a swimming fish can last for up to 5 min. Measurements were confined to a single layer and only one fish species, the goldfish *Carassius auratus*, to investigate: (1) how general the long duration of fish wakes is across species, (2) whether different fishes have different wake signatures that could possibly be discriminated by predators and (3) if the detection of hydrodynamic trails can be comparable or even superior to the use of other sensory systems operating in the dark, especially the acoustic system.

In this study, we used S-DPIV to measure and compare the long-term development of the wakes caused by three species of fish: the sunfish *Lepomis gibbosus*, the puffer *Colomesus psittacus* and the cichlid *Thysochromis ansorgii*. *Lepomis gibbosus* lives in the open water and in the reed zones of still temperate waters (Riehl and Baensch, 1991). Swimming manoeuvres include tail-propelled swimming and fast accelerations, although much of the locomotor time budget is accomplished by the pectoral fins. *Colomesus psittacus* lives in warm still water (Riehl and Baensch, 1991) and shows the typical tetraodontiform (Lindsey, 1978) swimming mode of a puffer, only in some cases the tail fin is used for propulsion. *Thysochromis ansorgii* is found in the peripheral zone of still and running waters (Riehl and Baensch, 1991). This fish tends to swim calmly with frequent use of the pectoral fins.

Materials and methods

Experimental animals

Two fish of each species *Lepomis gibbosus* L., *Colomesus psittacus* (Bloch & Schneider) and *Thysochromis ansorgii* (Boulenger), were obtained from commercial dealers and kept in standard aquaria according to the instructions in Riehl and Baensch (1991).

Experimental set-up and fish training

Two experimental tanks were used. Tank 1 had a floor surface of 100 cm×100 cm to give ample space for a lateral spread of the fish's wake. Tank 2 had a floor surface of 40 cm×100 cm to facilitate the laser illumination of the particles in the field of view and thus improve image quality. Image quality was highly dependent on the number of seeding particles that the laser light had to pass before it reached the area of interest. In both tanks the water level was set to 40±3 cm.

Individual fish were trained to swim on a straight line through the centre of the experimental tank to reach a goal compartment at the opposite wall where they received a food reward. Before a measurement the fish was kept in a small compartment at the start of the swimming route to allow the water in the experimental tank to calm down for at least 5 min. In training sessions the fish were conditioned to swim to a green light (a bright LED flashing at approximately 2 Hz). The light was mounted in the goal compartment at the lower end of a feeding tube, through which the fish was rewarded with a mosquito larva. As soon as the fish reached the goal compartment, it was locked out from the measurement area in the middle of the tank by shutting a sliding door.

To monitor the altitude of a swimming fish in side view, a third camera (camera 3) was positioned beside the experimental tank. The experimental tank was illuminated with green light to aid fish orientation. To avoid impairing the pictures taken by cameras 1 and 2, their object lenses were equipped with red filters. In initial experiments, a dim halogen lamp illuminated the fish while it was in the field of view, allowing to regain its kinematics from camera 1. In later experiments, an additional camera with a green filter (camera 4) was mounted above the experimental tank to improve image quality for kinematic analysis. Camera 4 was also synchronised with the light sheet illumination. Cameras 1, 2 and 4 were type DMK803 (The Imaging Source, Bremen, Germany); camera 3 was a surveillance camera (Conrad Electronic, Hirschau, Germany).

Flow measurements

A custom-made PIV device was used to measure the flow around and behind the freely swimming fish. Tracer particles (Vestosint 1101, Degussa AG, Marl, Germany) were seeded into the water and illuminated in six horizontal light sheets generated with modulated laser diodes (wavelength 650 nm, output power 50 mW) (Fig. 1). Vestosint is a synthetic material of density 1.02 g mm^{-2}. Median particle size was 74±5 μm (95%<147±5 μm). The light sheets were spaced equidistantly (vertical distance 10 mm for *Colomesus* and 12 mm for *Lepomis* and *Thysochromis*). The laser diodes were modulated using a micro-controller (Motorola 68HC05, Schaumburg, IL, USA) so that only one of the six planes was illuminated at a time, and the illuminated plane was switched to scan the water volume once in 12 video frames (equivalent to once per 0.48 s). Particle images were taken with one or two CCD cameras (termed cameras 1 and 2) mounted above the tank. Each camera had a chip size 768×582 pixels, frame rate was CCIR standard (50 half frames s^{-1}). The beginning of each half frame taken by the cameras was synchronised with the light sheet illumination. There was no need to adjust the focus of the cameras as light sheets were switched because the distance between the cameras and the light sheets exceeded tenfold the longest distance between light sheets. Pictures were stored on S-VHS video recorders (Philips VR1000, Eindhoven, The Netherlands) together with a synchronisation signal that served to determine the light sheet for each picture. Video frames were digitised using an MJPEG computer board (Miro Video DC30, Pinnacle Systems, Mountain View, CA, USA). The MJPEG board was set to a compression factor of 1:12, which does not affect the PIV results (Freek et al., 1999).

Data analysis

Since the cameras could only be synchronised to the start of a half frame, not a full frame, half frames were, if necessary,

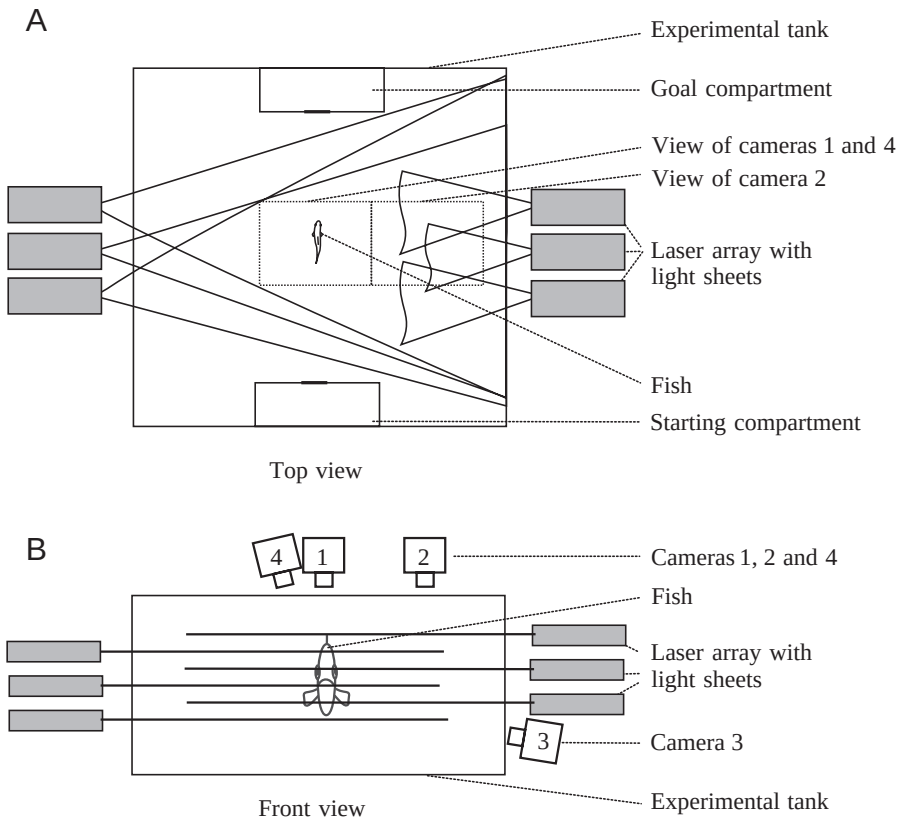

Fig. 1. Experimental set-up in (A) top view and (B) front view. Fish were trained to swim on a straight line through the middle of the experimental tank to reach a goal compartment where they received a food reward. Before a trial, an individual fish was kept in a starting compartment for at least 5 min. Six horizontal light sheets (thin illuminated layers of laser light) were installed in the middle of the tank. The water was seeded with neutrally buoyant particles. Cameras 1 and 2 recorded the movements of the seeding particles from above the tank. Cameras 3 and 4 recorded the fish's movements.

rearranged using Delphi 2.0 (Borland, Scotts Valley, CA, USA). Particle images were analysed using custom-made programs in MatLab 5.1 (The Mathworks, Natick, MA, USA). Analysis of particle displacement followed the principles of digital particle image velocimetry (Willert and Gharib, 1991), but was improved using the spurious vector detection technique described by Hart (2000). The interrogation area (the subimage that is subjected to the correlation procedure) was 32×32 pixels with an overlap of 50%, resulting in vector fields of 43×31 vectors. The images of the fish's silhouette from cameras 1 and 3 or cameras 4 and 3, respectively, were analysed manually using Scion Image (Scion Corporation, Frederick, MD, USA).

The analysis of fish-generated water disturbances is complicated by several specific problems. Firstly, water flow may be highly divergent and vortex structures may be small compared to the field of view. This makes the application of standard data post-processing procedures (e.g. Høst-Madsen and McCluskey, 1994; Westerweel, 1997; Hanke et al., 2000) undesirable. Where image quality was sufficient, which was the case in the narrow water tank (tank 2), we discarded post-processing of our velocity data. Velocity vectors were validated using three criteria. (1) The peak position criterion suggested by Hart (2000). Vectors were not used when the position of the first correlation peak in the product of two adjacent correlation planes differed from its position in each of the planes by more than 0.1 times the width of the interrogation area. (2) A peak height criterion. Vectors were assigned a status depending on the height of the correlation peak relative to its surrounding. (3) A velocity criterion. Velocity vectors that corresponded to a particle displacement of more than 0.3 times the width of an interrogation area and were out of the velocity range expected from comparison with similar measurements were discarded.

Secondly, the dynamic velocity range is very broad. The ratio of the highest to the lowest water velocities at a given point in time may easily reach an order of several hundred. This problem was solved by multiple-time-scale processing. Different time scales were not only used for different stages of the ageing of the water disturbances (cf. Hanke and Brücker, 1998), but also for different locations at a given point in time. Analysis started with a time spacing of 12 frames for each interrogation area, followed by a time spacing of 1.0 and 0.5 frames, depending on velocity and vector status information. Time spacing between 12 frames and 1 frame was not possible because of the scanning procedure (see above).

Thirdly, the fish moving through the camera's field of view is a foreign body, which can lead to false velocity information when using correlation techniques. This problem was solved by manually removing false vectors caused by the fish or its shadow using custom-made programs in Delphi 2.0 (Borland). Because our study focused on the long term development of the wake, the fish was in the field of view in less than 2% of the images.

Fourthly, in still water the fish's movements are generally not reproducible from trial to trial. This problem was overcome by the scanning technique, which allowed derivation of three-dimensional information from a single trial.

Statistical analysis

We compared the width of the trails caused by the three fish species using a *U*-test (e.g. Sachs, 1997) and the distribution of water velocities in the trails by comparing two trail indices TI1 and TI2, following the principles of discriminant analysis (e.g. Deichsel and Trampisch, 1985).

Results

Here we present four hydrodynamic trails of *Lepomis gibbosus*, three trails of *Colomesus psittacus* and three trails of *Thysochromis ansorgii* measured in the narrow tank (tank 2). In addition we describe two trails of *Thysochromis ansorgii* measured in the broad tank (tank 1). To evaluate the 12 trails over a time span of 5 min, a total of 63 000 video frames was analysed.

In Fig. 2, the silhouette of a *Lepomis* is shown as it moved through the field of view. For clarity, the fish silhouettes were shifted laterally; the curved line connecting circles in the centre of the figure indicates the position of the fish's head in successive images.

The water movements caused in this trial are plotted as velocity vector fields and the corresponding divergence in Fig. 3A,B (A, after approximately 10 s; B, after approximately 60 s). The time of each vector field is indicated in its upper right corner; t=0 s is the time when the fish entered the field of view. Times of different vector fields are slightly different because of the scanning procedure. The number of the illuminated layer is indicated in the upper left corner of each vector field, where 1 designates the uppermost, 6 the lowermost layer (spacing between layers was 12 mm). Velocity is indicated by the 10 mm s^{-1} and 2 mm s^{-1} scale bars in A and B, respectively, and the spatial extent by the 100 mm scale bars. Divergence, represented by different colours (see colour bar), is defined as $(d/dx)\cdot v_x+(d/dy)\cdot v_y$ and indicates the flow out of or into a small section of the plane (x and y are the cartesian coordinates, v_x and v_y are the x and y components of the velocity). We show the divergence because it gives an impression of the out-of-plane water movements that could not be measured directly in this study, but should be relevant to a predator's sensory system (Bleckmann, 1994).

It is apparent from this example that the trail of *Lepomis gibbosus* can show a clear vortex structure for at least 60 s (Fig. 3B). Vortices have slightly grown after 60 s compared to those after 10 s (Fig. 3A), but are still in the length scale of the wake generator's body.

Fig. 4A–C shows the development of water flow characteristics over 60 s for this *Lepomis* trial (Fig. 4A), for a *Colomesus* trial (Fig. 4B) and a *Thysochromis* trial (Fig. 4C). Maximum water velocity (top), mean water velocity (middle) and maximum amount of vorticity (bottom) are shown. Vorticity is plotted because it is associated with velocity gradients that fish can detect with their lateral line (Bleckmann, 1994). In each plot, the values for all six laser light sheets are shown in different colours. The fish silhouette with horizontal lines indicate the position of the fish relative to the light sheets.

It is apparent from Fig. 4A–C that the maximum velocity (top) and vorticity (bottom) in all three trials decayed rapidly within the first 10 s, but nevertheless persisted considerably longer than that. The same was true for the mean velocity in *Lepomis* (4A, centre). Mean velocities in *Colomesus* (4B, centre) and *Thysochromis* (4C, centre) decayed even slower (relative to their starting values, which were lower than in *Lepomis*). Differences between the various layers could be substantial for maximum and mean velocity as well as for maximum vorticity (Fig. 4A–C).

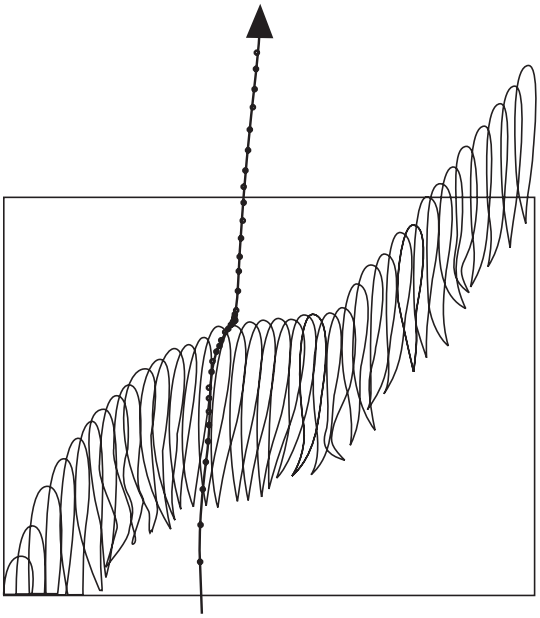

Fig. 2. Silhouette of *Lepomis gibbosus* as it swam through the field of view. For clarity, the silhouettes were shifted laterally; the curved line connecting circles in the centre of the figure indicates the position of the fish's head in successive images.

Table 1 shows water velocity values in representative layers and a description of the fish's movements for each of the 12 trials that were evaluated. The amounts of water velocity before the trial, after 5 s and after 60 s (where t=0 s is the time when the fish entered the field of view) are given as median, maximum and upper and lower quartile. t_{end} in Table 1 designates the time when the upper quartile returned to starting conditions; velocity values are given for this time or for 300 s, respectively.

The spatial extent of six fish trails measured in tank 2 in representative layers is shown in Fig. 5. To visualise the development of the trails, the amount of water velocity was averaged over the columns of each vector field and the rows resulting from this procedure were assembled in temporal order. Water velocity is colour coded. Note that the colour scale does not cover the full range of velocities (see Table 1 and Figs 3, 4) in order to resolve the low velocities in the aged trail.

It is apparent from Fig. 5 that the spatial extent and temporal structure of the trails from *Lepomis* and *Thysochromis* can be distinguished from the *Colomesus* trails in their lateral spread. The portions of a fish wake that spread laterally are mainly produced by undulating body movement, lateral tail flicks and pectoral fin movements, while *Colomesus* mainly used an tetraodontiform swimming style (dorsal and anal fin undulations). Accordingly, the *Colomesus* trails show essentially one narrow zone of water disturbance, while the trails of the other two species divide in two or more branches. Water velocities caused by the small *Colomesus* were lower

Table 1. *Characteristic features of fish-generated water disturbances for three species with a description of the swimming behaviour*

	Velocity (mm s^{-1})													Velocity (mm s^{-1}) at t_{end} or t=300 s					Swim speed (mm s^{-1})		
	Before trial				After 5 s				After 60 s												
Species (*BL*)	i	ii	iii	iv	i	ii	iii	iv	i	ii	iii	iv	t_{end} (s)	i	ii	iii	iv	Figs	Min.	Average	Max.
Lepomis gibbosus (86±1 mm)																					
Trial 1	0.09	0.13	0.18	0.41	0.26	0.81	1.37	2.33	0.31	0.60	0.98	2.05	>300	0.10	0.16	0.26	0.44	2, 3A,B, 4A, 5A, 6	19	185	501
Trial 2	0.10	0.14	0.20	0.35	0.47	0.83	1.29	2.34	0,19	0.41	0.74	1.74	278	0.07	0.12	0.20	0.39	5B, 6	245	446	554
Trial 3	0.06	0.10	0.13	0.23	0.50	0.83	1.13	2.30	0.19	0.32	0.64	1.55	>300	0.09	0.15	0.20	0.33	6	37	269	566
Trial 4	0.07	0.10	0.14	0.23	0.11	0.27	0.66	2.02	0.14	0.24	0.43	1.78	257	0.06	0.09	0.14	0.29	6	172	337	415
Colomesus psittacus (38±1 mm)																					
Trial 5	0.22	0.40	0.64	0.91	0.25	0.49	0.76	1.94	0.20	0.42	0.64	0.99	47	0.23	0.43	0.64	1.10	4B, 5C, 6	63	153	353
Trial 6	0.16	0.26	0.41	0.67	0.59	0.81	1.14	2.31	0.15	0.23	0.38	0.76	40	0.16	0.27	0.41	0.88	5D, 6	36	120	317
Trial 7	0.15	0.23	0.36	0.66	0.18	0.32	0.49	1.46	0.19	0.30	0.49	1.47	85	0.16	0.26	0.36	0.66	6	53	156	356
Thysochromis ansorgii (86±1 mm)																					
Trial 8	0.21	0.31	0.42	0.79	0.27	0.49	0.81	1.88	0.31	0.47	0.65	1.24	272	0.11	0.25	0.42	0.79	4C, 5E, 6	94	132	171
Trial 9	0.13	0.21	0.37	0.65	0.17	0.41	0.65	1.51	0.22	0.41	0.64	1.02	>300	0.16	0.30	0.50	0.68	5F, 6	117	142	168
Trial 10	0.12	0.20	0.38	0.64	0.11	0.20	0.43	1.99	0.19	0.33	0.53	0.95	184	0.20	0.29	0.38	0.58	6	78	110	152
Trial 11	0.13	0.18	0.25	0.44	0.13	0.22	0.42	1.56	0.15	0.26	0.39	0.95	175	0.09	0.16	0.25	0.47		113	159	276
Trial 12	0.10	0.14	0.22	0.49	0.16	0.24	0.46	1.75	0.11	0.21	0.41	0.96	194	0.09	0.14	0.22	0.54		37	67	99

BL, body length.

Maximum water velocity in this table is defined as the mean amount of the 67 (=5%) longest velocity vectors.

The amount of water velocity before the trial, after 5 s and after 60 s (where t=0 s is the time when the fish entered the field of view) is given as lower (i) median (ii) and upper (iii) quartiles and maximum (iv). t_{end} is the time when the upper quartile returned to starting conditions; velocity values (i–iv) to the right of t_{end} apply to t_{end} or to 300 s in cases where t_{end} exceeded 300 s.

Trials 1–4, *Lepomis gibbosus.* (1) Entered field of view gliding fast; nearly stopped in the centre; accelerated with two tail flicks. Change of altitude 20±5 mm. (2) Entered field of view undulating constantly; decelerated in the second half; accelerated leaving field of view. Constant altitude (±10 mm). (3) Entered field of view undulating constantly; decelerated substantially in the second half; accelerated leaving field of view. Constant altitude (±10 mm). (4) Entered field of view undulating constantly; decelerated when leaving field of view; constant altitude (±10 mm).

Trials 5–7, *Colomesus psittacus.* (5) Mainly dorsal and anal fins used, steering with tail fin (tetraodontiform swimming). Two half flicks of tail fn in the last quarter. Constant altitude (±10 mm). (6) Mainly dorsal and anal fins used, steering with tail fin (tetraodontiform swimming). Acceleration in the last quarter aided by the tail fin. Change of altitude 20±5 mm. (7) Mainly dorsal and anal fins used, steering with tail fin (tetraodontiform swimming). Deceleration in the first quarter. Acceleration in the last quarter aided by the tail fin. Change of altitude 20±10 mm.

Trials 8–12, *Thysochromis ansorgii.* (8) Change of direction of 20° aided by left pectoral fin, followed by fast tail flick aided by pectoral fins, low amplitude undulation aided by pectoral fins, low-amplitude undulation and spreading of pectoral fins. Change of altitude 30±5 mm. (9) Constant low amplitude motions of tail fin, four strokes of pectoral fins, straight swimming path. Change of altitude 20±5 mm. (10) Low amplitude motions of tail fin, six strokes of pectoral fins; curved swimming path. (11) Low amplitude motions of tail fin, three strokes of pectoral fins; straight swimming path. (12) Low amplitude motions of tail fin, seven strokes of pectoral fins; curved swimming path.

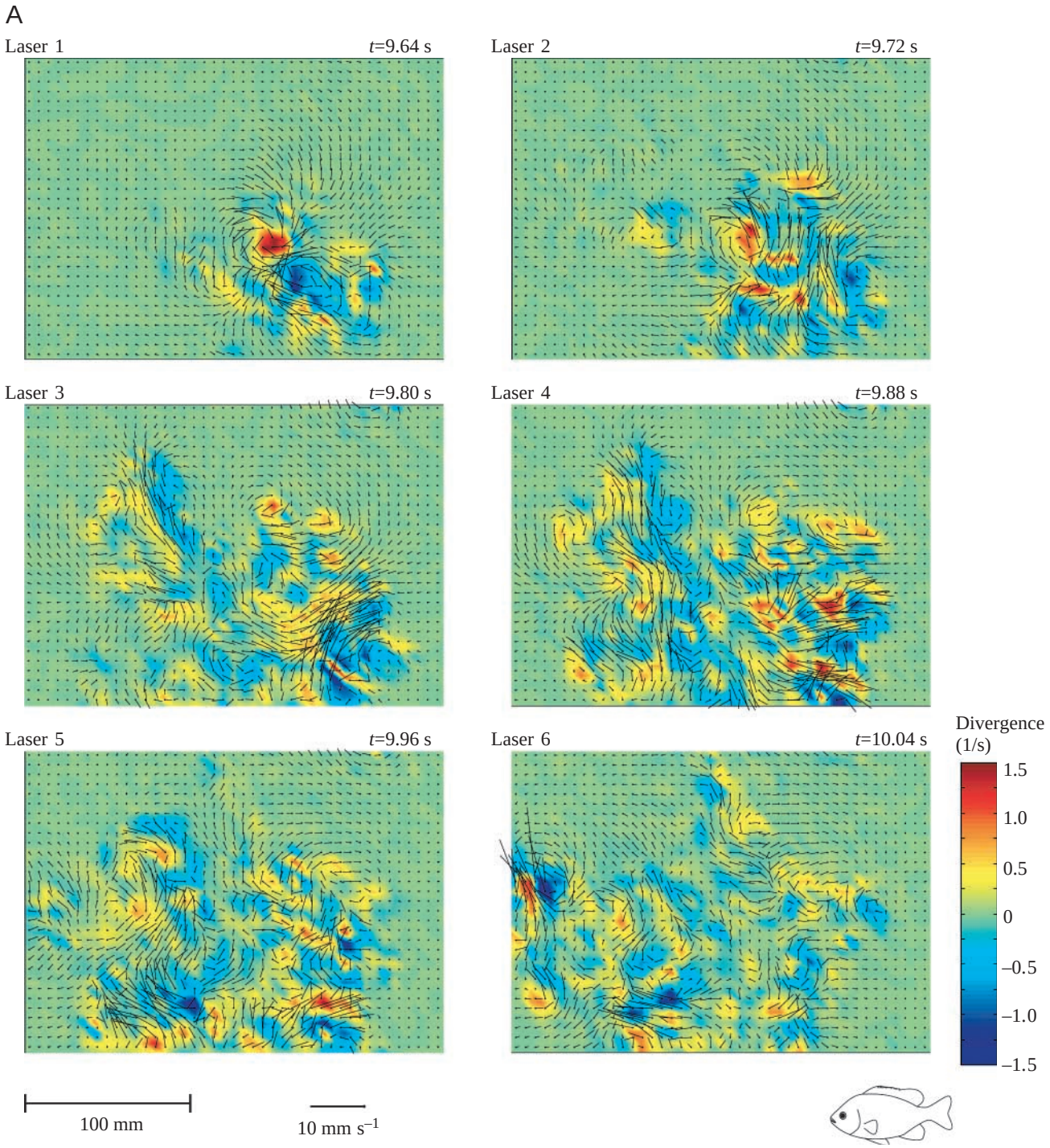

Fig. 3. (A,B) Fish wake of *Lepomiss gibbosus* in six layers as velocity vector fields. The different layers are indicated by the laser number in the upper left corner of each vector plot, where laser 1 illuminated the uppermost and laser 6 the lowermost layer. The illuminated layers were spaced equidistantly (12 mm apart). Water velocities and divergence are shown at $t\approx10$ s (A) and $t\approx60$ s (B) (t=0 s is the time when the fish entered the field of view; times of vector fields are slightly different because of the scanning procedure). Divergence is defined as $(d/dx)\cdot v_x + (d/dy)\cdot v_y$ (x and y are the cartesian coordinates, v_x and v_y are the x and y components of the velocity) and indicates the flow out of or into a small section of the plane, which is caused by out-of-plane movements.

than the water velocities caused by the other two species (note the different velocity scales).

Table 2 adds information on the lateral spread for the five layers that are not shown in Fig. 5 and for the remaining trials. The width of each fish wake at t=10 s and t=20 s in all six layers is given. It is defined as the width of the zone where the water velocity calculated as in Fig. 5 was at least 0.8 mm s^{-1}. If the trail reached the border of the field of view in *Lepomis*,

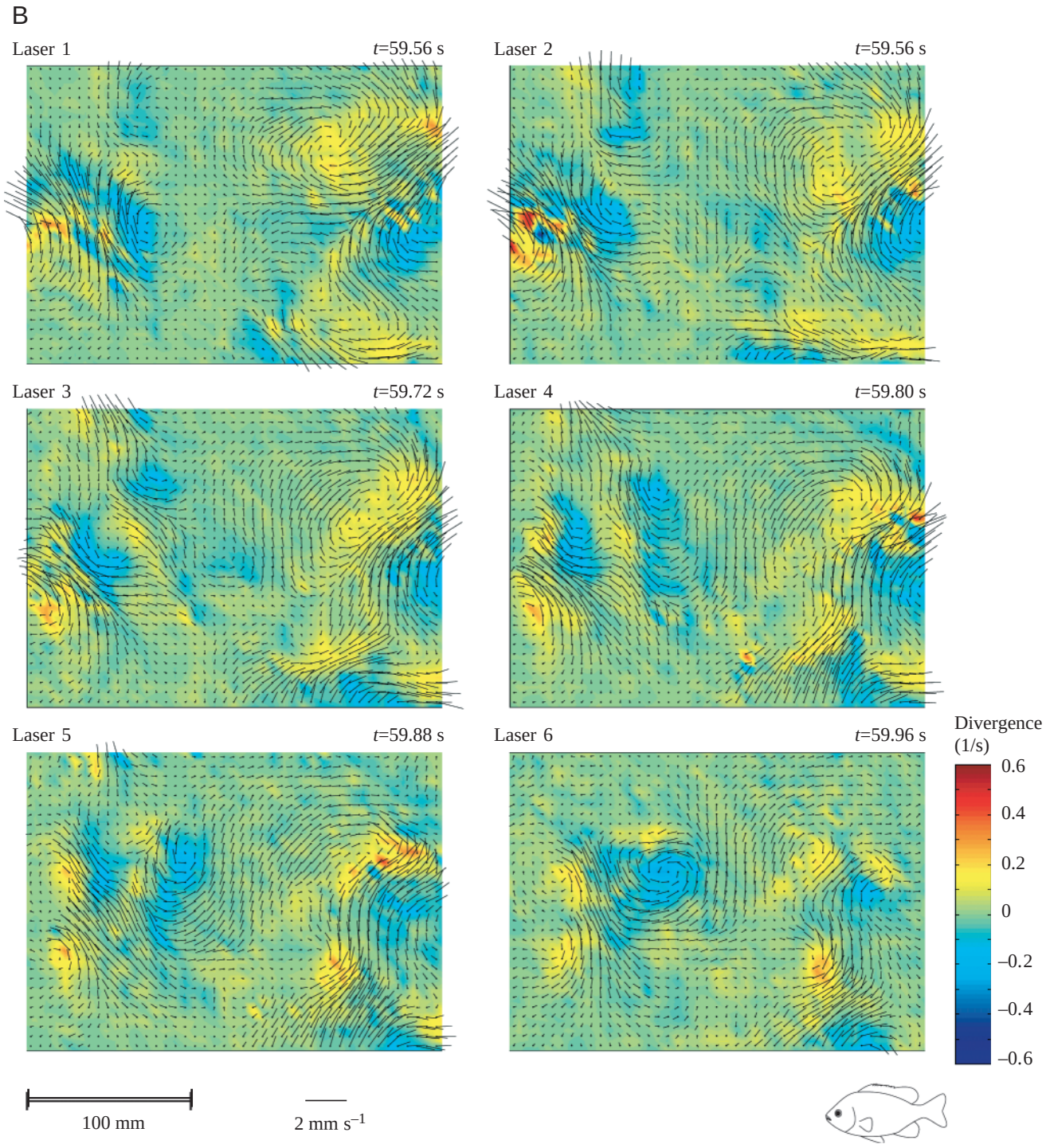

lower boundaries are given (e.g. width >262 mm), and in *Thysochromis*, trail width was estimated by extrapolation (marked with *). In trials 4, 11 and 12, trail width was estimated as twice the width on one side of the fish because swim paths were close the border of the field of view. Where no width was calculated, water velocity did not reach 0.8 mm s^{-1}. Comparing the maximal width (replaced by its lower limit if the border of the field of view was reached) in all the trials shows a clear difference between species in these trials (*U*-test, α=0.05).

The trails of *Lepomis*, *Colomesus* and *Thysochromis* can be distinguished visually by the distribution of velocity over their cross section (Fig. 5). The *Lepomis* trails appear more sharp-contoured compared to the more diffuse *Thysochromis* trails. It must be noted that in these trials *Lepomis* performed exclusively fast swimming manoeuvres (see Table 1 and Discussion).

Table 3 supports this visual impression numerically. We defined two trail indices, TI_1 and TI_2. To calculate TI_1 and TI_2 for each trial from tank 2, the vector field at t≈10 s was

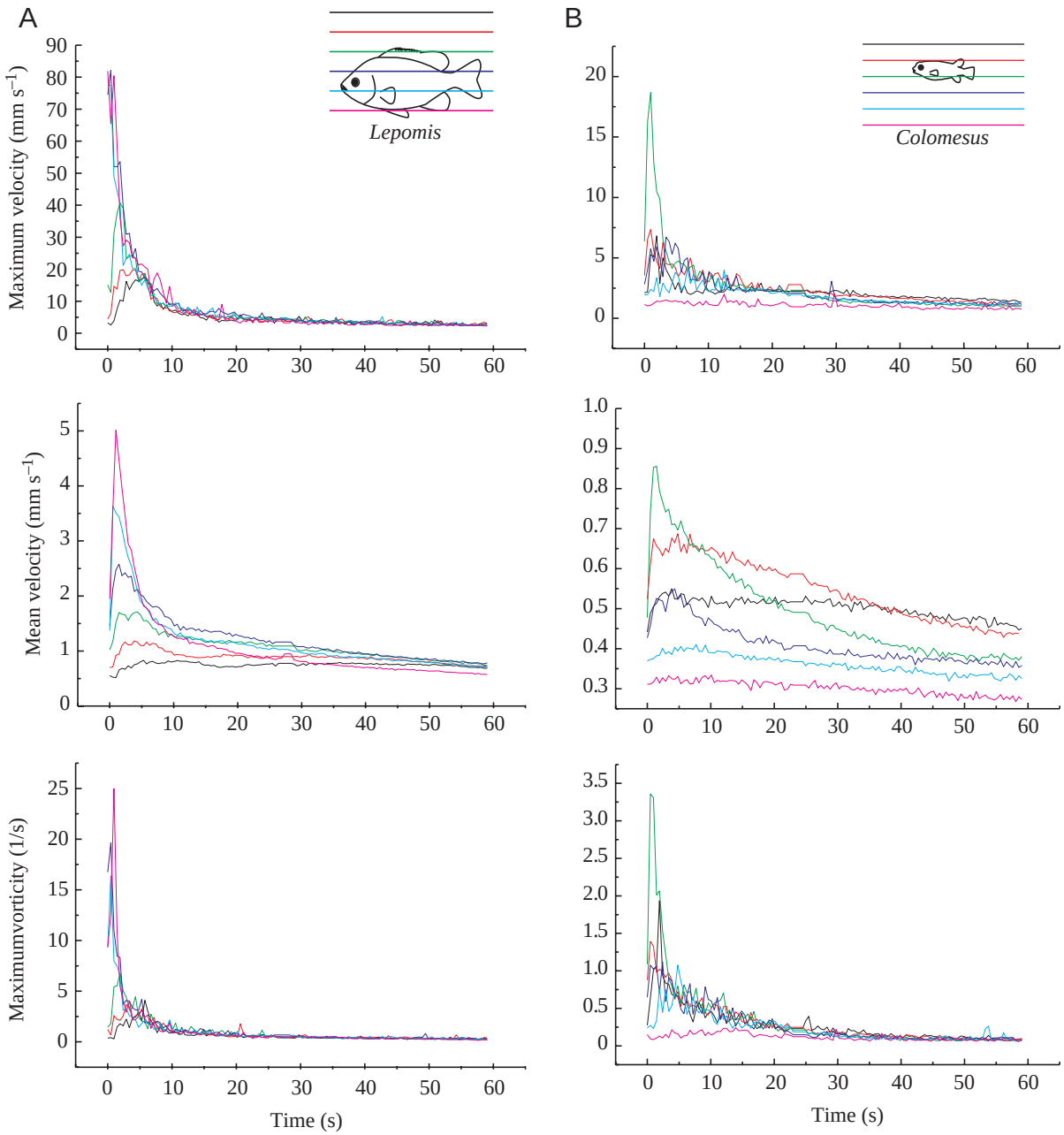

Fig. 4. (A–C) Velocity and vorticity values for one trial with *Lepomis* (A), one trial with *Colomesus* (B) and one with *Thysochromis* (C) as function of time (60 s). Maximum velocity in the field of view (top), mean velocity in the field of view (middle) and maximum vorticity in the field of view (bottom) are shown. Different colours refer to different layers (black, layer 1 = uppermost layer; red, layer 2; green, layer 3; blue, layer 4; cyan, layer 5; magenta, layer 6 = lowermost layer.

reduced to a row by averaging the amount of velocity over its columns as in Fig. 5. The result was a curve c(x) that showed the average water velocity as a function of lateral position x at t≈10 s. To make this comparison independent of the velocity differences between species, c(x) was normalized by setting its maximum velocity value to 1, yielding a curve c1(x). The curve c1(x) was then smoothened by a moving average filter (width n=29), resulting in a curve c2(x). TI_1 is the number of intersections of c1(x) and c2(x). TI_2 is the maximum of c2(x)–c1(x). Both TI_1 and TI_2 were averaged over all laser light sheets that touched the tail fin of the fish in the centre of the field of view.

The trail indices from Table 3 are plotted in Fig. 6. The trails of different species tend to form clusters, with the *Colomesus* cluster rather distinct from the other species. Only one *Lepomis* trail with TI_1=3, TI_2=0.356 comes close to *Colomesus*. It must be noted that in this *Lepomis* trial, the fish did not swim through the centre of the field of view but close to its border, so that a considerable part of the wake was lost for analysis. The wakes of *Lepomis* and *Thysochromis* are not intermingled; however,

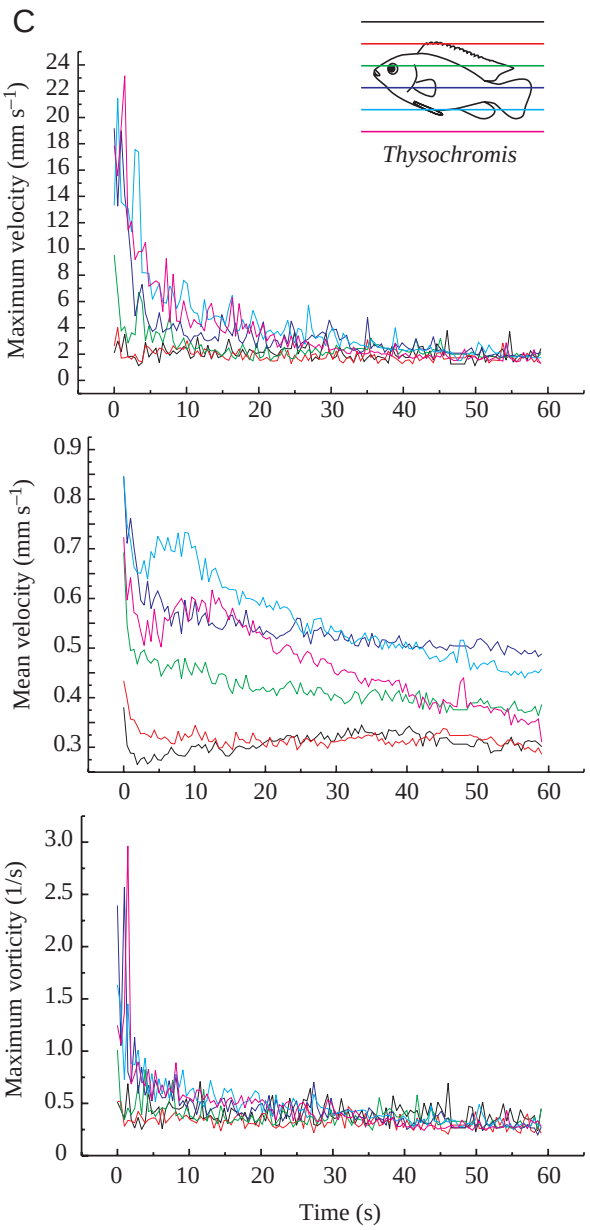

intraspecific distance can be higher than interspecific distance. Discriminant analysis and the estimation of error rates using the leaving-one-out-method (L-method, e.g. Deichsel and Trampisch, 1985) yields an error rate of 20%. This is reduced to 12% if the Lepomis trail with TI_1=3, TI_2=0.356 is omitted.

Discussion

Our measurements of water disturbances generated by swimming fish yield insight into the flow patterns caused by three species that differed in swimming style. It was found that, similar to the goldfish trails (Hanke et al., 2000), the water disturbances caused by these species can last in the order of minutes (or at least for about 30 s in the case of *Colomesus*), even in water with thermal convection currents (see Table 1).

Selection of tank and tank width

Animal-generated flow is often difficult to study because it is usually neither reproducible nor stationary or two-dimensional. To achieve reproducibility, fish were forced to swim in a flow tank (for references, see Drucker and Lauder, 2003). This method is appropriate if one is interested in the structure of the wake measured close to the fish. However, if one is interested in the ageing of fish-generated wakes, flow tanks are usually too short. Furthermore, they add a certain degree of turbulence to the water that can override weak flow structures. The use of S-DPIV in still water copes with these problems.

All of our measurements were therefore done in still water tanks. To improve image quality (see Materials and methods) and thus reduce the number of unreliable vectors, which in our wide tank could be as high as 25% compared to 1% in the narrow tank, most measurements were performed in the narrow tank (tank 2). The disadvantage of the narrow tank is that its walls may have restricted the lateral spread of the fish's wake or changed its structure. In *Lepomis*, a portion of the wake usually reached the border of the field of view, equivalent to two thirds of the width of tank 2, in a short time (Fig. 5A). However, the clear vortex structures of the fish wakes even after 60 s in *Lepomis* that can be seen in Fig. 3 and the lateral spread of the wakes of *Thysochromis* (Fig. 5C, narrow tank) compared with the data from the broad tank (Table 1) led us to believe that the wall effect can be small in some swimming manoeuvres. On the other hand, a lateral spread of a goldfish's wake that exceeded 50 cm has been reported elsewhere (Hanke et al., 2000). Hence tank width should always be adapted to the specific question asked.

Hydrodynamic wake detection

Our data show that even small fish produce wakes that can indicate the presence of the wake generator for at least 0.5–5 min, depending on body length and swimming style. This makes fish-generated wakes a potential source of information for piscivorous fish (cf. Pohlmann et al., 2001) and mammals (cf. Dehnhardt et al., 2001). While wake-following behaviour in the viscous length scale of planktonic organisms has been attributed to chemoreception (Yen et al., 1998), in the swimming fish range of Reynolds number the mechanical component of the wake is an additional cue that fish cannot easily avoid.

Why should the detection of hydrodynamic trails with mechanosensory systems be comparable or even superior to the use of other sensory systems operating in the dark, especially the acoustic system? Consider a prey fish that swims in a manner similar to the *Lepomis* in our trial 2 (Table 1). With an average speed of 44.6 cm s^{-1} (5.2 body length s^{-1}; Table 1), it can cover a range of more than 25 m within 1 min. The hydrodynamic trail after 1 min still contains velocities higher than 1.7 mm s^{-1} (Table 1), which are above the detection threshold of the lateral line (Görner, 1963). To estimate the acoustic field produced by a small fish 25 m away, we substitute the tail fin by a dipole and use the dipole equations quoted by Kalmijn (1988). This approximation is justified as long as the fish does not change its volume, i.e. the monopole moment is

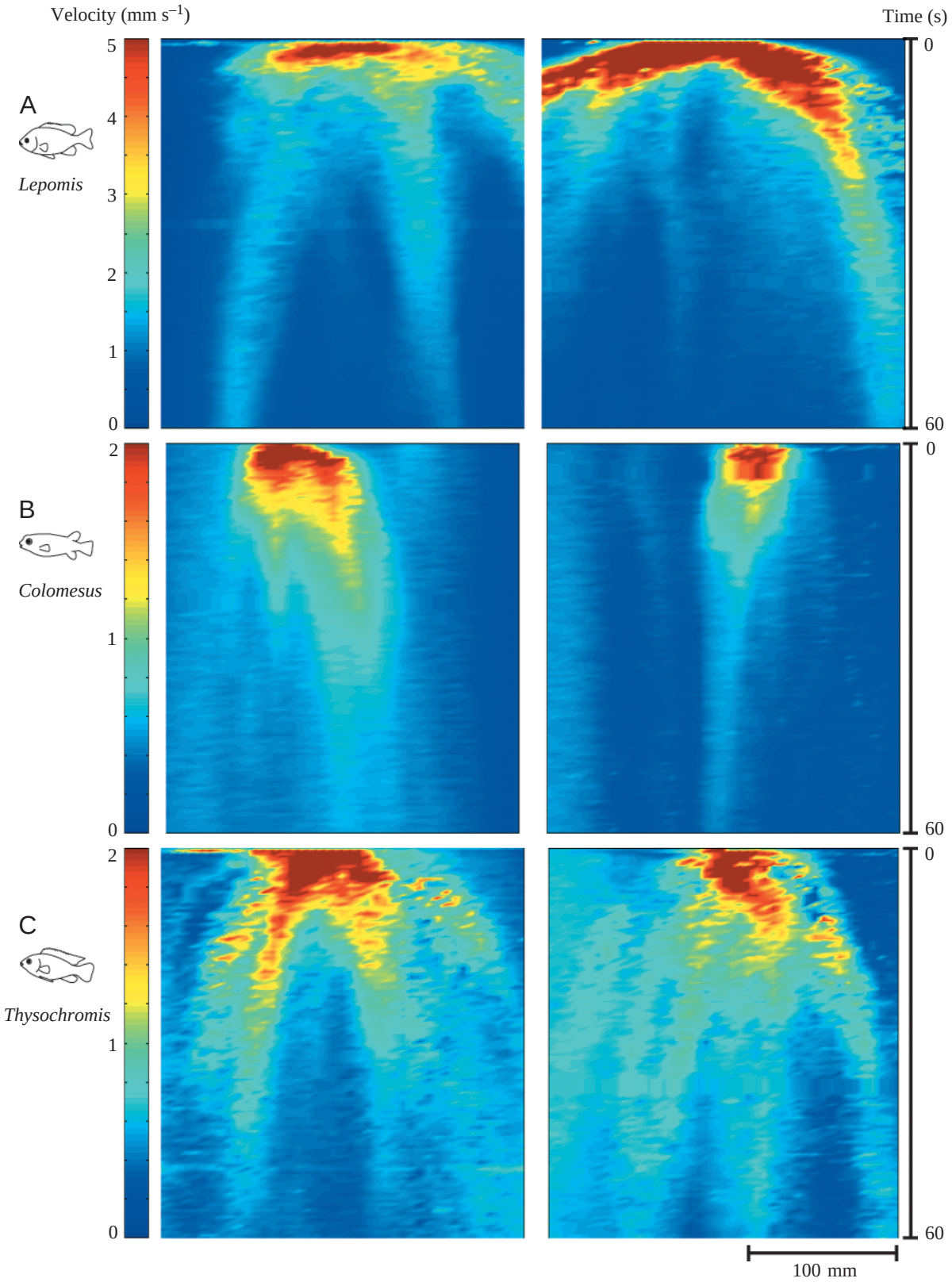

Fig. 5. Visualisation of the spatial extent of the fish's wakes. For this figure, each vector field was reduced to a row by averaging over the columns of the vector field, and the rows resulting from this procedure were assembled in temporal order. Note that the velocity scale does not cover the complete range of measured values (cf. Figs 3, 4 and Table 1) in order to resolve the low velocities in the aged trail. A shows two *Lepomis* wakes, B shows two *Colomesus* wakes and C shows two *Thysochromis* wakes (see Table 1 for survey of trials).

Table 2. *Width of the fish trails at 10 s and 20 s after the passage of the fish in six layers for all trials*

	Width of trail (mm)											
	After 10 s						After 20 s					
Species	Layers 1 → 6						Layers 1 → 6					
Lepomis gibbosus												
Trial 1	120	139	188	190	>216	>225	97	209	211	214	192	>219
Trial 2	None	None	>183	>244	>259	>262	None	None	194	>244	>259	>262
Trial 3	47	221	>237	>233	>248	>252	>42	>245	>248	>252	>255	>258
Trial 4	119	156	182	197	161	25	80	197	235	261	228	30
Colomesus psittacus												
Trial 5	27	101	91	121	6	None	33	106	74	40	12	None
Trial 6	71	50	51	40	12	18	10	6	6	23	None	None
Trial 7	None	None	None	56	59	72	None	None	None	87	100	90
Thysochromis ansorgii												
Trial 8	12	12	30	109	178	180	None	None	None	121	147	130
Trial 9	163	171	137	127	67	68	203*	177	185	139	39	74
Trial 10	82	148	143	133	13	None	59*	77	190*	164	24	None
Trial 11	156	158	194	186	165	156	167	180	229	209	188	191
Trial 12	167	180	217	186	176	180	194	192	240	197	188	192

Velocity vector fields were reduced by taking the mean of each vector column. Then the width of each trail was calculated with the border of the trail defined as 0.8 mm s^{-1}. If the trail reached the border of the field of view in *Lepomis*, lower boundaries are given (e.g. width >262 mm), and in *Thysochromis*, trail width was estimated by extrapolation (*). In trials 4, 11 and 12, trail width was estimated as twice the width on one side of the fish.

zero; the quadrupole and higher moments fall off with the distance much faster than the dipole moment. Assuming a dipole radius of 10 mm, an oscillation amplitude of 10 mm and an oscillation frequency of 5 Hz, the water velocity produced by the dipole at a distance of 25 m is as small as 1.8×10^{-11} m s^{-1}, and the corresponding acceleration amplitude is 3.1×10^{-10} m s^{-2}. The hearing threshold of a typical piscivorous predator, the perch *Perca fluviatilis*, is in the order of 10^{-4} m s^{-2} (Karlsen, 1992). Thus while the hydrodynamic sensory system most probably responds to the hydrodynamic trail, acoustic perception of the prey is impossible in this example. The same calculation with the *Thysochromis* data from trial 12 (see Table 1, lowest average swimming speed of all trials presented – this may be closer to the fish's routine speed than the *Lepomis* speeds are) leads to a distance of more than 4 m covered by the fish in 1 min. The dipole in our model causes an acceleration amplitude of 1.5×10^{-7} m s^{-2} at a distance of 4 m, which is again well below the hearing threshold of the predator. The hydrodynamic trail contained water velocities of 0.96 mm s^{-1} and would most probably be sensed.

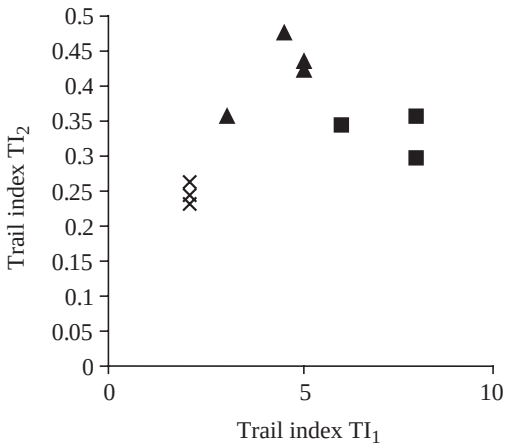

Fig. 6. The trails from tank 2 related to their trail indices TI_1 and TI_2 (see text and Table 3). *Lepomis*, triangles; *Colomesus*, crosses; *Thysochromis*, squares.

We do not know how often the high swimming speeds of *Lepomis* observed in our experiments (average up to 5.2 *BL* s^{-1}, where *BL is* body length) occur in nature. Due to experimental constraints *Lepomis*, like all other fish, was trained to swim to a flashing light where it expected a food reward. In this situation, high swimming speeds represented the spontaneous behaviour of our *Lepomis*. In nature the upper range of swimming speeds may well be reached in various situations including defending a breeding or feeding territory, reproductive interactions or predator–prey interactions. A 10 cm goldfish *Carassius auratus* can reach 11.4 *BL* s^{-1} for 0.1 min (Tsukamoto et al., 1975). In addition, the results from the fast-swimming *Lepomis* give a first estimate for the wakes of fast-swimming fish that have not been investigated yet. Prolonged speeds in a 25 cm herring *Clupea harengus* were 5.5 *BL* s^{-1} for 3 min (He and Wardle, 1988; Videler, 1993).

It has not been shown that the hydrodynamic wake of a prey fish unequivocally reveals the species or the swimming style to a predator. However, in the examples presented here, wake

Table 3. *Trail indices TI_1 and TI_2 for all trials from tank 2*

Species	Trail index TI_1	Trail index TI_2
Lepomis gibbosus		
Trial 1	5	0.435
Trial 2	5	0.421
Trial 3	4.5	0.476
Trial 4	3	0.356
Colomesus psittacus		
Trial 5	2	0.261
Trial 6	2	0.244
Trial 7	2	0.232
Thysochromis ansorgii		
Trial 8	6	0.344
Trial 9	8	0.298
Trial 10	8	0.357

To calculate TI_1 and TI_2, the vector field at $t \approx 10$ s was reduced to a row by averaging the amount of velocity over its columns as in Fig. 5. The result is a curve $c(x)$ that shows the average water velocity as a function of lateral position x at $t \approx 10$ s. $c(x)$ was divided by its maximum to normalize the curve; the resulting curve was called $c1(x)$. $c1(x)$ was smoothened by a moving average filter (width $n=29$), resulting in a curve $c2(x)$. TI_1 is the number of intersections of $c1(x)$ and $c2(x)$. TI_2 is the maximum of $c2(x)–c1(x)$. Both TI_1 and TI_2 were averaged over all laser light sheets that touched the tail fin of the fish in the centre of the field of view.

patterns were diverse (Figs 3, 5, 6), while vortex structures in the length scale of the flow-generating structures were observed (Fig. 3). Since many hydrodynamic sensory systems measure water flow in multiple points (Bleckmann, 1994), it is likely that a predator can extract information beyond the mere presence of a wake and learn to interpret such flow structures to a certain degree.

We thank Dr G. Dehnhardt for supplying part of the video equipment. The work reported herein was supported by a grant of the Deutsche Forschungsgemeinschaft to H.B. (Bl 242/9-1).

References

Adrian, R. J. (1991). Particle imaging techniques for experimental fluid mechanics. *Annu. Rev. Fluid Mech.* **23**, 261-304.

Baker, C. F. and Montgomery, J. C. (2002). The sensory basis of rheotaxis in the blind Mexican cave fish, *Astyanax fasciatus*. *J. Comp. Physiol. A* **184**, 519-527.

Bleckmann, H. (1994). *Reception of Hydrodynamic Stimuli in Aquatic and Semiaquatic Animals*. Stuttgart, Jena, New York: Fischer.

Bleckmann, H., Mogdans, J. and Dehnhardt, G. (2001). Lateral line research: the importance of using natural stimuli in studies of sensory systems. In *Ecology of Sensing* (ed. F. G. Barth and A. Schmid), pp. 149-167. Berlin: Springer-Verlag.

Bleckmann, H., Tittel, G. and Blübaum-Gronau, E. (1989). The lateral line system of surface feeding fish: Anatomy, physiology and behavior. In *The Mechanosensory Lateral Line. Neurobiology and Evolution* (ed. S. Coombs, P. Görner and H. Münz), pp. 501-526. New York: Springer-Verlag.

Dehnhardt, G., Mauck, B., Hanke, W. and Bleckmann, H. (2001). Hydrodynamic trail following in harbor seals (*Phoca vitulina*). *Science* **293**, 102-104.

Deichsel, G. and Trampisch, H. J. (1985). *Clusteranalyse und Diskriminanzanalyse*. Stuttgart, New York: Fischer.

Drucker, E. G. and Lauder, G. V. (1999). Locomotor forces on a swimming fish: three-dimensional vortex wake dynamics quantified using digital particle image velocimetry. *J. Exp. Biol.* **202**, 2393-2412.

Drucker, E. G. and Lauder, G. V. (2000). A hydrodynamic analysis of fish swimming speed: wake structure and locomotor force in slow and fast labriform swimmers. *J. Exp. Biol.* **203**, 2379-2393.

Drucker, E. G. and Lauder, G. V. (2001). Locomotor function of the dorsal fin in teleost fishes: experimental analysis of wake forces in sunfish. *J. Exp. Biol.* **204**, 2943-2958.

Drucker, E. G. and Lauder, G. V. (2003). Function of pectoral fins in rainbow trout: behavioral repertoire and hydrodynamic forces. *J. Exp. Biol.* **206**, 813-826.

Freek, C., Sousa, J. M. M., Hentschel, W. and Merzkirch, W. (1999). On the accuracy of a MJPEG-based digital image compression PIV-system. *Exp. Fluids* **27**, 310-320.

Görner, P. (1963). Untersuchung zur Morphologie und Elektrophysiologie des Seitenlinienorgans vom Krallenfrosch *Xenopus laevis*. *J. Comp. Physiol. A* **47**, 316-338.

Hanke, W. and Brücker, C. (1998). The time course of a goldfish's vortex street measured and analyzed with a custom made PIV device. *Fachtagungen der Deutschen Gesellschaft für Laseranemometrie GALA e. V.* no. 6 (ed. W. Merzkirch, F. Peters, B. Ruck, D. Dopheide and A. Leder), pp. 51-57. Aachen: Shaker-Verlag.

Hanke, W., Brücker, C. and Bleckmann, H. (2000). The ageing of the low-frequency water disturbances caused by swimming goldfish and its possible relevance to prey detection. *J. Exp. Biol.* **203**, 1193-1200.

Hart, D. P. (2000). PIV error correction. *Exp. Fluids* **29**, 13-22.

He, P. and Wardle, C. S. (1988). Endurance at intermediate swimming speeds of Atlantic mackerel, *Scomber scombrus* L., herring, *Clupea harengus* L., and Saithe, *Pollachius virens* L. *J. Fish Biol.* **33**, 255-266.

Høst-Madsen, A. and McClusky, D. A. (1994). On the accuracy and reliability of PIV measurements. *Seventh International Symposium on the Application of Laser Techniques to Fluid Mechanics*, pp. 1-11. Lisbon.

Kalmijn, A. J. (1988). Hydrodynamic and Acoustic Field Detection. In *Sensory Biology of Aquatic Animals* (ed. J. Atema, R. R. Fay, A. N. Popper and W. N. Tavolga), pp. 83-130. New York: Springer-Verlag.

Karlsen, H. E. (1992). The inner ear is responsible for detection of infrasound in the perch (*Perca fluviatilis*). *J. Exp. Biol.* **171**, 163-172.

Lindsey, C. C. (1978). Form, function and locomotory habits. In *Fish Physiology. Vol. VII: Locomotion* (ed. W. S. Hoar and D. J. Randall), pp. 1-100. New York: Academic Press.

Müller, U. K., Stamhuis, E. J. and Videler, J. J. (2000). Hydrodynamics of unsteady fish swimming and the effects of body size: comparing the flow fields of fish larvae and adults. *J. Exp. Biol.* **203**, 193-206.

Müller, U. K., van den Heuvel, B. L. E., Stamhuis, E. J. and Videler, J. J. (1997). Fish foot prints: morphology and energetics of the wake of a continuously swimming mullet. *J. Exp. Biol.* **200**, 2893-2906.

Nauen, J. C. and Lauder, G. V. (2002). Quantification of the wake of rainbow trout (*Oncorhynchus mykiss*) using three-dimensional stereoscopic digital particle image velocimetry. *J. Exp. Biol.* **205**, 3271-3279.

Pohlmann, K., Grasso, F. W. and Breithaupt, T. (2001). Tracking wakes: The nocturnal predatory strategy of piscivorous catfish. *Proc. Natl. Acad. Sci. USA* **98**, 7371-7374.

Riehl, R. and Baensch, H. A. (1991). *Aquarien-Atlas*. Hong Kong: Mergus.

Sachs, L. (1997). *Angewandte Statistik*. Berlin, Heidelberg, New York: Springer-Verlag.

Stamhuis, E. J. and Videler, J. J. (1995). Quantitative flow analysis around aquatic animals using laser sheet particle image velocimetry. *J. Exp. Biol.* **198**, 283-294.

Tsukamoto, K., Kajihara, T. and Nishiwaki, M. (1975). Swimming ability of fish. *Bull. Jap. Soc. Sci. Fish* **41**, 167-174.

Videler, J. J. (1993). *Fish Swimming*. London, Weinheim, New York, Tokyo: Chapman & Hall.

Westerweel, J. (1997). Fundamentals of digital particle image velocimetry. *Meas. Sci. Technol.* **8**, 1379-1392.

Willert, C. E. and Gharib, M. (1991). Digital particle image velocimetry. *Exp. Fluids* **10**, 181-193.

Yen, J., Weissburg, M. J. and Doall, M. H. (1998). The fluid physics of signal perception by mate-tracking copepods. *Philos. Trans. R. Soc. Lond. B* **353**, 787-804.